Clathrin heavy chain mediates TACC3 targeting to mitotic spindles to ensure spindle stability

Chiou-Hong Lin,[1,2] Chi-Kuo Hu,[3,4] and Hsiu-Ming Shih[1,2]

[1]Graduate Institute of Life Sciences, National Defense Medical Center, and [2]Institute of Biomedical Sciences, Academia Sinica, Taipei 11529, Taiwan
[3]Department of Systems Biology and [4]Graduate Program in Biological and Biomedical Sciences, Harvard Medical School, Boston, MA 02115

Mitotic spindles play essential roles in chromosome congression and segregation during mitosis. Aurora A regulates spindle assembly in part via phosphorylating human TACC3 on S558, which triggers TACC3 relocalization to mitotic spindles and stabilizes microtubules (MTs). In this study, we identified clathrin heavy chain (CHC) as an adaptor protein to recruit S558-phosphorylated TACC3 onto the spindle during mitosis for MT stabilization. CHC binds phospho-S558 TACC3 via its linker domain and first CHC repeat. CHC depletion or mutation on phospho-TACC3 binding abrogates TACC3 spindle relocalization. Depletion of either or both CHC and TACC3 yields similar defective phenotypes: loss of ch-TOG on spindles, disorganized spindles, and chromosome misalignment with comparable mitotic delay. Our findings elucidate the association between aurora A phosphorylation and spindle apparatus and demonstrate that regulation from aurora A is mediated by CHC in recruiting phospho-TACC3 and subsequently ch-TOG to mitotic spindles.

Introduction

Proper organization of bipolar mitotic spindles ensures the fidelity of chromosome segregation during cell division (Kline-Smith and Walczak, 2004). Aurora A is a key mitotic kinase regulating spindle function via phosphorylation of a variety of proteins (Giet et al., 1999, 2002; Wong et al., 2008). Among its substrates, TACC3 (transforming acidic coiled-coil–containing protein 3) has recently emerged as an important player in organizing mitotic spindles (Kinoshita et al., 2005; Pascreau et al., 2005; Peset et al., 2005; Peset and Vernos, 2008). Aurora A phosphorylates TACC3 on S558, which facilitates TACC3 localization to spindles and subsequently ch-TOG recruitment, promoting microtubule (MT) assembly (Brittle and Ohkura, 2005; Barr and Gergely, 2007). Notably, TACC3 depletion causes MT destabilization and chromosome misalignment (Gergely et al., 2003; Schneider et al., 2007), resembling some aberrant mitotic events of cells with aurora A disruption (Marumoto et al., 2003; Sasai et al., 2008). Furthermore, treatment of a selective aurora A inhibitor precluded TACC3 localization to the spindle (LeRoy et al., 2007), correlating with the formation of abnormal mitotic spindles (Hoar et al., 2007). Thus, it is conceivable that the capacity of TACC3 in spindle association is crucial for MT stabilization. Although phosphorylation of TACC3 S558 by aurora A is essential for its spindle localization, the molecular mechanism underlying TACC3 phosphorylation-dependent spindle targeting remains elusive.

In addition to being a component of clathrin involved in coating various transport vesicles for protein trafficking (Schmid, 1997), clathrin heavy chain (CHC) is concentrated on the spindle during mitosis and stabilizes the MT fibers (Okamoto et al., 2000; Royle et al., 2005; Yamauchi et al., 2008). CHC depletion causes destabilized kinetochore fibers, defective chromosome congression, and prolonged mitosis (Royle et al., 2005). Although CHC is also required for mitotic spindle function, the mechanism by which CHC regulates spindle stability is unclear. In this study, we show that CHC mediates phospho-TACC3 interaction and spindle recruitment and also provide a model for CHC stabilization of mitotic spindles.

Results and discussion

Identification of CHC as a phospho-S558 TACC3–interacting protein

To identify factors capable of binding to phospho-S558 TACC3, GST-TACC3 522–577 fusion proteins, consisting of TACC3

The Rockefeller University Press $30.00
J. Cell Biol. Vol. 189 No. 7 1097–1105
www.jcb.org/cgi/doi/10.1083/jcb.200911120

JCB **1097**

Figure 1. CHC associates with phospho-S558 TACC3. (A) The SYPRO ruby gel shows CHC pulled down from Noc-treated HeLa cell extracts by recombinant GST-TACC3 522–577 fusion proteins phosphorylated by recombinant aurora A. CHC peptides detected by mass spectrometry are indicated. (B) Western blotting shows CHC pulled down by recombinant GST-TACC3 proteins phosphorylated by aurora A. Input represents the 5% amount of Noc-treated HeLa cell extracts subjected to the pull-down assays. Coomassie blue staining shows various GST fusion proteins used for each binding reaction. The phosphorylation levels of GST-TACC3 proteins in kinase reactions are shown by autoradiography. (C–E) Western blots show complex formation of endogenous TACC3 and CHC by immunoprecipitation (IP) with the indicated antibodies from mitotic HeLa cells synchronized by Noc (C), from Noc-synchronized cells with or without additional treatment of 2 µM VX-680 (D), or from Noc-synchronized cell lysates with or without treatment of λ-phosphatase (λPPase) before being subjected to immunoprecipitation (E). The phospho-T288 level correlates to aurora A kinase activity. Input represents the 5% amount of the indicated lysates for each immunoprecipitation. Black lines indicate that intervening lanes have been spliced out. (F and G) Representative images of HeLa cells in metaphase stained with DNA (blue) and antibodies against α-tubulin or CHC (green) and TACC3 (H-300) or phospho-TACC3 (pTACC3; red) are shown. Bars, 10 µm.
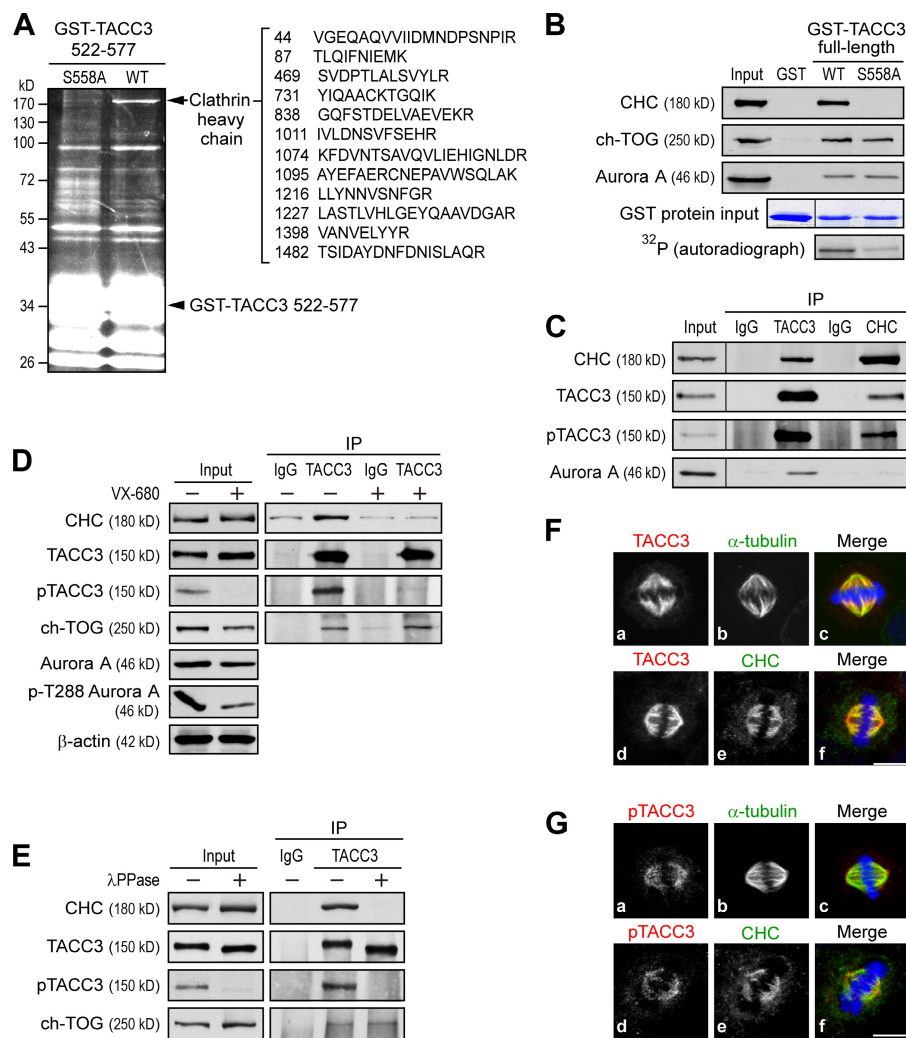
amino acid residues 522–577, were phosphorylated by aurora A kinase in vitro and subjected to pull-down assays with nocodazole (Noc)-arrested extracts from HeLa cells. GST-TACC3 522–577 wild type (WT) but not S558A mutant pulled down a distinct band with a molecular mass >170 kD (Fig. 1 A). Mass spectrometry analysis suggested that this band represented CHC. We further substantiated the specificity of CHC to phospho-S558 TACC3 in the full-length context of TACC3. The GST-S558A mutant showed a marked decrease in both aurora A–mediated phosphorylation and CHC precipitation compared with WT (Fig. 1 B). Under the same binding conditions, the levels of pulled-down ch-TOG and aurora A from mitotic extracts were similar in S558A and WT (Fig. 1 B), which is consistent with data demonstrating that TACC3 binds to both ch-TOG and aurora A via its TACC domain (Lee et al., 2001; unpublished data). These results indicate that the CHC–TACC3 interaction occurs specifically via phospho-S558 of TACC3 and excludes the involvement of any other potential aurora A phosphorylation sites of TACC3 during CHC interaction. Of note, the phosphorylation at S558 by itself was crucial for CHC interaction because phosphorylation-mimic S558D or S558E failed to efficiently pull down CHC protein (Fig. S1 A). Accordingly, TACC3

S558D or S558E was defective in spindle association, similar to S558A (Fig. S1 B).

We further verified the phospho-S558–dependent interaction between TACC3 and CHC at an endogenous level. Coimmunoprecipitation experiments with mitotic HeLa cells revealed that endogenous CHC, similar to aurora A, could be precipitated by TACC3 (Fig. 1 C). Reciprocal immunoprecipitation showed TACC3 in the CHC immunocomplex by antibodies against TACC3 or phospho-S626 of maskin (Pascreau et al., 2005), a *Xenopus laevis* homologue of TACC3 (Fig. 1 C). The specificity of this phospho antibody (phospho-TACC3) in recognizing human TACC3 phospho-S558 was confirmed by Western analysis (Fig. S2 A). Furthermore, aurora A was barely precipitated by CHC, implying that CHC may not associate with aurora A. Notably, treatment of HeLa cells with aurora kinase inhibitor VX-680 (before cell harvest) or treatment of cell lysates with λ-phosphatase (before coimmunoprecipitation) markedly diminished phospho-S558 levels, which correlated with a decreased level of CHC precipitated by TACC3 (Fig. 1, D and E). In contrast, the interaction between TACC3 and ch-TOG was insensitive to VX-680 or λ-phosphatase treatment. Together, these results suggest that endogenous CHC–TACC3 interaction is S558 phosphorylation dependent.

We further examined the intracellular localizations of phospho-S558 TACC3 and CHC in mitotic cells. Both TACC3 and CHC colocalized at spindles in metaphase (Fig. 1 F). Similar to a regular TACC3 antibody, the phospho-TACC3 antibody yielded clear signals with mitotic spindles and CHC (Fig. 1 G). This is different from a previous study using another phospho-maskin/TACC3 antibody (Kinoshita et al., 2005), which showed that phospho-TACC3 mainly localizes to centrosomes. We compared both phospho-maskin/TACC3 antibodies and revealed that the phoshpo-TACC3 antibody (provided by Y. Arlot-Bonnemains, University of Rennes, Rennes, France; Pascreau et al., 2005) gave a higher degree of specificity in immunofluorescence analysis (Fig. S2, B and C). The phospho-TACC3 antibody decorated the spindle correlated well with the results of S558 mutants defective in spindle association (Fig. S1) and with a selective aurora A inhibitor, which excluded TACC3 localization to the spindle (LeRoy et al., 2007).

CHC is crucial for TACC3 spindle association

We next tested the interdependence between TACC3 and CHC on spindle localization. Depletion of TACC3 by siRNA did not alter CHC association with the spindle (Fig. 2 A, d). In contrast, CHC depletion rendered a striking loss of TACC3 from spindles as detected by anti-TACC3 (Fig. 2 A, h, n, and q) or phospho-TACC3 antibody (Fig. 2 B, e and k). Fig. 2 C showed the level of TACC3 spindle recruitment in siRNA-treated cells, which was quantified and normalized to MT intensity because CHC depletion affected spindle stability (see Materials and methods). Of note, CHC depletion neither altered aurora A localization and activity nor affected the level of phospho-S558 TACC3 (Fig. 2, D and E), indicating that TACC3 spindle mislocalization in siCHC-treated cells was unrelated to the process of TACC3 phosphorylation by aurora A. Together, these results suggest that CHC serves as an adaptor to recruit phospho-S558 TACC3 onto spindles. In line with this notion, the results of in vitro aster assembly and MT-binding experiments showed that depletion of CHC rendered a dramatic loss of the association of phospho-S558 TACC3 (or TACC3) proteins with MTs, whereas aurora A or Eg5 was not affected (Fig. 2 F).

CHC is required for TACC3-associated spindle regulation

Having shown that CHC mediates TACC3 spindle targeting, we knocked down CHC to explore whether CHC plays a role in TACC3-dependent mitotic phenotype. CHC and/or TACC3 were depleted >90% by specific siRNAs compared with control sample (siGL2; Fig. 3 A). Under such conditions, CHC-depleted cells, similar to TACC3-depleted cells, exhibited a threefold higher mitotic index than control cells (Fig. 3 B). About 70% of mitotic cells showed prolonged progress from chromosome condensation onset to anaphase onset (siCHC and siTACC3, 120 and 135 min; control cells, 40 min; Fig. 3 C and Video 1), and the remainder failed to proceed to anaphase over the 5-h observation period (Video 2). Moreover, aberrant chromosome alignment during mitosis in CHC- or TACC3-depleted cells was also observed (Fig. 3 D, arrows). More importantly,

when cells were simultaneously depleted of both CHC and TACC3, the mitotic index, mitotic delay, and chromosome alignment defects were not further elevated compared with CHC- or TACC3-depleted cells (Fig. 3, B, C, and E, lane 4), implicating that both CHC and TACC3 function in a similar if not identical fashion in mitosis.

Aberrant spindle formation is often accompanied by abnormal chromosomal arrangement. In line with this notion, we observed highly disorganized spindles and reduced MT content with thicker metaphase plate in CHC- and/or TACC3-depleted cells (Fig. 4 A). Accordingly, the levels of aberrant spindles in both CHC–TACC3-depleted cells were similar to those of cells depleted with either CHC or TACC3 alone (Fig. 4 B). In addition to our data showing CHC recruitment of TACC3 to the spindle (Fig. 2), the aberrant spindles caused by CHC depletion would likely be associated with a defect in TACC3 recruitment.

Because TACC3 recruits ch-TOG to promote MT assembly (Kinoshita et al., 2005; Peset et al., 2005), it is possible that CHC is also involved in spindle regulation via the recruitment of TACC3–ch-TOG complexes. We first showed that endogenous ch-TOG could be precipitated by CHC (Fig. 4 C) and further observed that depletion of CHC resulted in a loss of ch-TOG localization to the spindle but not to the centrosome (Fig. 4 D, e), which is similar to that observed in siTACC3-treated cells shown in Fig. 4 D or in previous studies (Gergely et al., 2003; Barr and Gergely, 2008). Notably, CHC depletion caused a phenotype of disrupted K fibers, as indicated by staining of hepatoma upregulated protein (Fig. 4 F), which correlated with a loss of ch-TOG function on K fiber regulation (Barr and Gergely, 2008). In contrast, the staining pattern of other MT-associated proteins, such as astrin, was not significantly disturbed in siCHC cells (unpublished data), suggesting that the effect of CHC depletion on spindle mislocalization of ch-TOG was specific. Notably, the phenomenon of ch-TOG–defective spindle localization in both CHC–TACC3-depleted cells was similar to that observed in cells depleted either for TACC3 or CHC alone (Fig. 4, D and E). These results suggest that CHC and TACC3 are in the same pathway axis for recruiting ch-TOG, further supporting the notion that CHC mediates the spindle targeting of TACC3.

Because ch-TOG is important for MT polymerization and stabilization, in line with the implication of CHC in spindle recruitment of ch-TOG, we observed similar defects in MT repolymerization after cold shock in siCHC- and/or siTACC3-treated cells (Fig. 4 G); the defective phenotypes in MT staining intensity and spindle length caused by CHC and/or TACC3 depletion were also further quantified (Fig. 4 H). These results not only further substantiate that both CHC and TACC3 are required for spindle stabilization, but they also provide a possible mechanism by which CHC regulates spindle assembly via the recruitment of TACC3–ch-TOG complexes to the spindle.

Domain mapping of CHC for TACC3 phospho-S558 interaction

To further elucidate the role of CHC in recruiting TACC3 onto spindles, we delineated the domain of CHC involved in phospho-TACC3 interaction by pull-down assays and revealed that the 331–542 fragment, which is comprised of a linker region and the
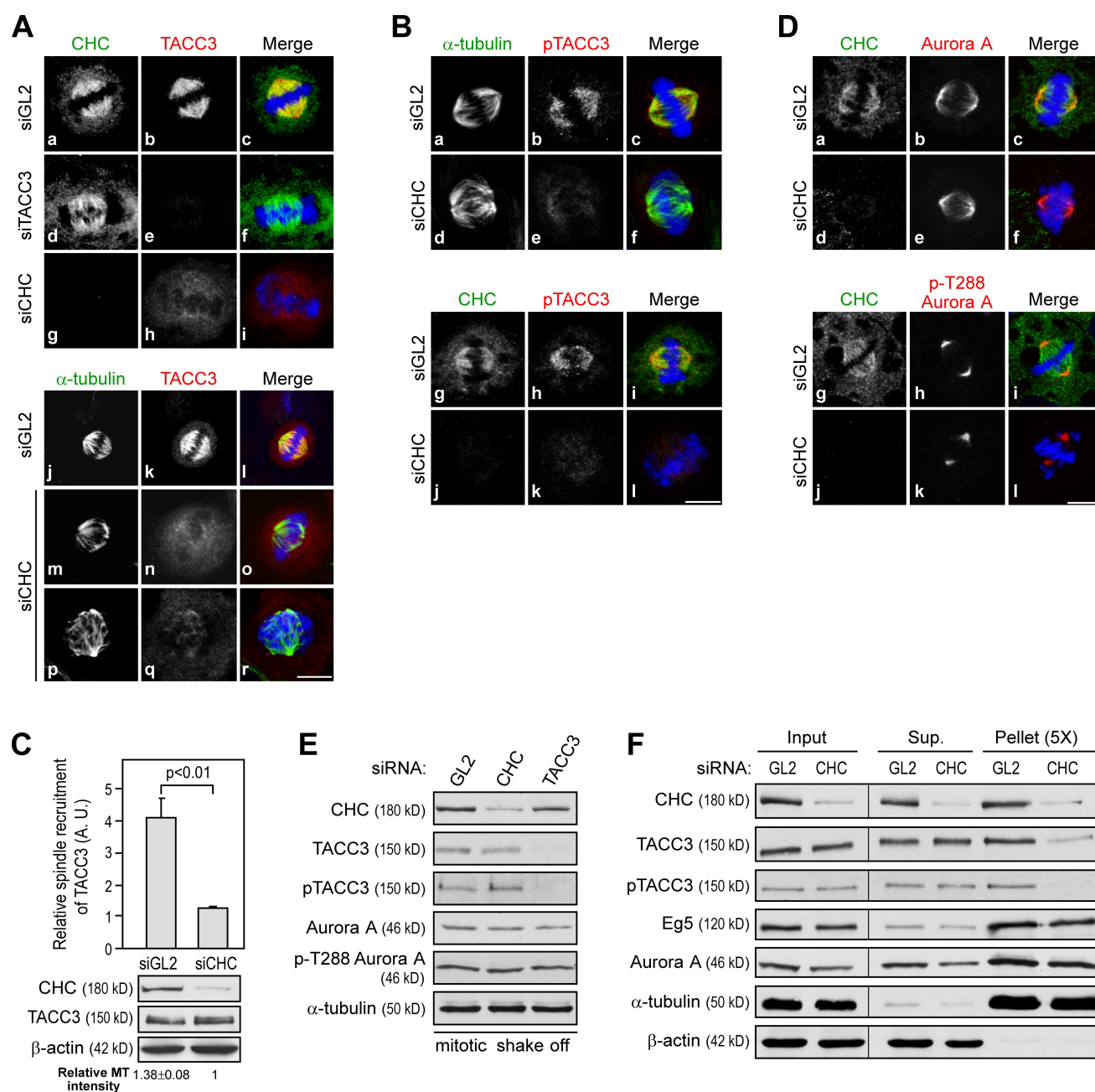
Figure 2. **CHC is essential for TACC3 localization to the spindle.** (A, B, and D) Metaphase images of HeLa cells treated with the indicated siRNAs for 72 h and stained with DNA (blue), TACC3 (H-300), phospho-TACC3 (pTACC3), aurora A, or phospho-T288 aurora A (red) and CHC or α-tubulin (green) as indicated. Bars, 10 µm. (C) Histogram shows TACC3 recruitment to the spindle in HeLa cells treated with the indicated siRNAs. Expression levels of the indicated proteins in siRNA-treated cells are shown. Relative spindle recruitment and spindle MT intensity are quantified as described in Materials and methods. Error bars indicate mean ± SD (n = 3; >20 mitotic cells scored per experiment). (E and F) Western blots show the levels of indicated proteins from mitotic extracts of cells treated with indicated siRNAs (E) and the level of indicated proteins from in vitro aster and MT-binding assays with mitotic extracts of cells treated with the indicated siRNAs (F). Black lines indicate that intervening lanes have been spliced out. Sup, supernatant.

first CHC repeat CHCR0, was sufficient for phospho-TACC3 interaction (Fig. 5, A and B [arrowhead]). The importance of this segment for phospho-TACC3 association was further indicated by reciprocal pull-down assays using a CHC mutant internally deleting residues 331–542 (Fig. 5 C).

If CHC mediates TACC3 spindle targeting, the CHC mutant defective in TACC3 interaction should lose the capacity to recruit TACC3 to the spindle. To test this, we depleted endogenous CHC in HeLa cells by siRNA followed by transfection of

Flag-tagged CHC WT or Δ(331–542) mutant engineered to be insensitive to CHC siRNA treatment. The CHC Δ(331–542) mutant retained the spindle association (Fig. 5 D), although to a lesser degree than that of WT (Fig. 5 E). Under such conditions, the CHC Δ(331–542) mutant failed to recruit TACC3 to the spindle compared with CHC WT (Fig. 5 F, h). Similarly, ch-TOG was not localized on the spindle in CHC Δ(331–542)–transfected cells (Fig. 5 G, h). These results demonstrate a correlation between the interaction and spindle recruitment of
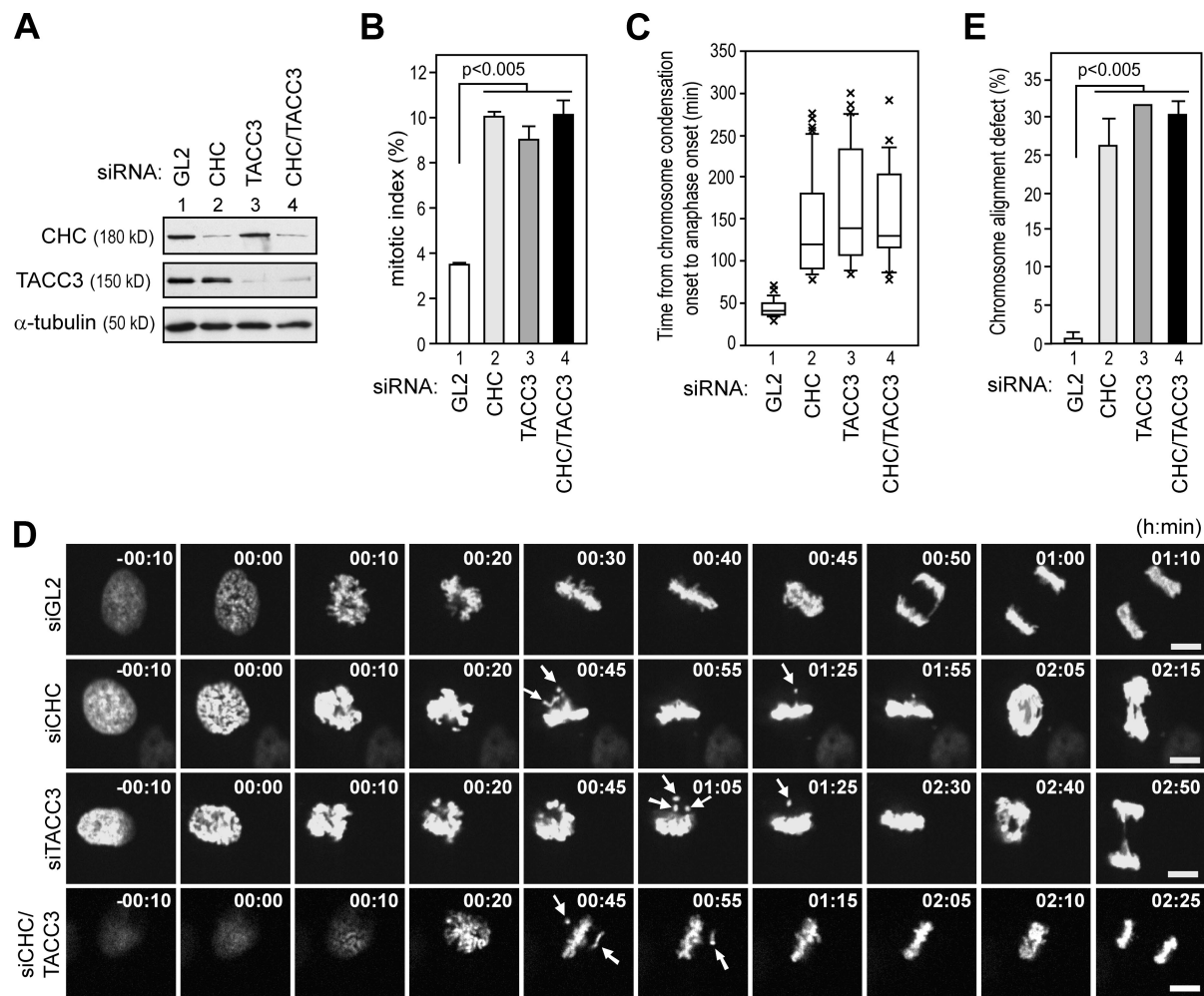
Figure 3. Depletion of CHC and/or TACC3 causes comparable mitotic delay and chromosome alignment defect. (A) Western blotting shows the expression levels of CHC and TACC3 in HeLa cells treated with the indicated siRNAs. (B) Bar graph shows mitotic index of HeLa cells treated with the indicated siRNAs ($n = 3$; >500 cells scored per condition). (C) Box and whisker plot measuring time spent in mitosis of HeLa cells expressing GFP-H2B treated with the indicated siRNAs (>25 cells scored per condition; $P < 0.0001$). (D) Still images from Video 1 of HeLa cells expressing GFP-H2B treated with the indicated siRNAs are shown. Arrows show chromosome misalignment. Bars, 10 µm. (E) Bar graph shows the percentage of mitotic HeLa cells with a metaphase-like plate and misaligned chromosome after treatment of the indicated siRNAs ($n = 3$; ~100 cells per experiment). Error bars indicate mean ± SD.

TACC3 by CHC, further supporting the role of CHC in recruiting the TACC3–ch-TOG complex to spindles. Defective spindle recruitment of TACC3–ch-TOG also resulted in mitotic defects such as increased mitotic index and chromosome misalignment in CHC Δ(331–542)–transfected cells (Fig. 5, H and I).

Previous studies of CHC suggested that CHC could bundle MTs using its triskelia structure and that the N-terminal fragment 1–542 fused to the C-terminal trimerization domain is the minimal structural requirement for the function of clathrin in mitosis (Royle et al., 2005; Royle and Lagnado, 2006). Although the C-terminal and N-terminal 1−330 domains were defined for trimer formation and mitotic spindle attachment, respectively, the role of the CHC 331–542 segment in mitosis was unknown. Our findings that the 331–542 region mediates TACC3 spindle recruitment provide an important insight to account for the function of such a small CHC fragment in mitosis. Furthermore, the results that the Δ(331–542) mutant failed to confer CHC function in mitosis also suggest that both N-terminal spindle attachment and C-terminal triskelion for bundling MTs

are necessary but insufficient to support the function of CHC in spindle stabilization.

Although our study demonstrated that CHC directly interacts with phopsho-TACC3 (Fig. 5) and is required for phospho-TACC3 targeting to spindles (Fig. 2), the mechanism regarding how CHC recruits phospho-TACC3 to spindle MTs remains unclear. Notably, recombinant TACC3 with or without phosphorylation was unable to bind to MTs directly by in vitro MT-binding assays (Fig. S3). This is distinct from the property of *Xenopus* maskin protein, which is able to bind directly to MTs (O'Brien et al., 2005; Peset et al., 2005). We attempted to demonstrate the recruitment of recombinant phospho-TACC3 proteins to MTs via the recombinant CHC protein. However, the recombinant CHC protein itself failed to bind MTs (Fig. S3), implying that some accessory factors and/or posttranslational modifications may be required for CHC to associate with MTs in mitosis. Indeed, a recent study suggested that transcription factor B-Myb in complex with filamin is required for CHC localization to spindles (Yamauchi et al., 2008). However, B-Myb–filamin complex

Figure 4. Depletion of CHC and/or TACC3 renders a loss of ch-TOG spindle targeting and aberrant spindles. (A, D, and F) Images of HeLa cells treated with the indicated siRNAs and stained with DNA (blue), α-tubulin or CHC (green), and ch-TOG or hepatoma up-regulated protein (HURP; red) as indicated are shown. (B) Bar graph shows quantification of aberrant spindle morphology of cells as observed in A (n = 3; >100 cells per experiment). (C) Western blots show complex formation of endogenous CHC and ch-TOG by immunoprecipitation (IP) with the indicated antibodies from mitotic HeLa cells. Input represents the 5% amount of Noc-treated cell extracts subjected to immunoprecipitation. Black lines indicate that intervening lanes have been spliced out. (E) Bar graph shows the recruitment of ch-TOG to the spindle of cells observed in D (n = 3; >10 mitotic cells scored per experiment). (G) Images of MT repolymerization after cold shock of the indicated siRNA-treated cells. Cells were fixed and stained with α-tubulin (green) and DNA (blue). (H) Bar graph shows MT intensity and half-spindle length of cells observed in G (n = 3; >20 mitotic cells scored per experiment). Error bars indicate mean ± SD. Bars, 10 µm.
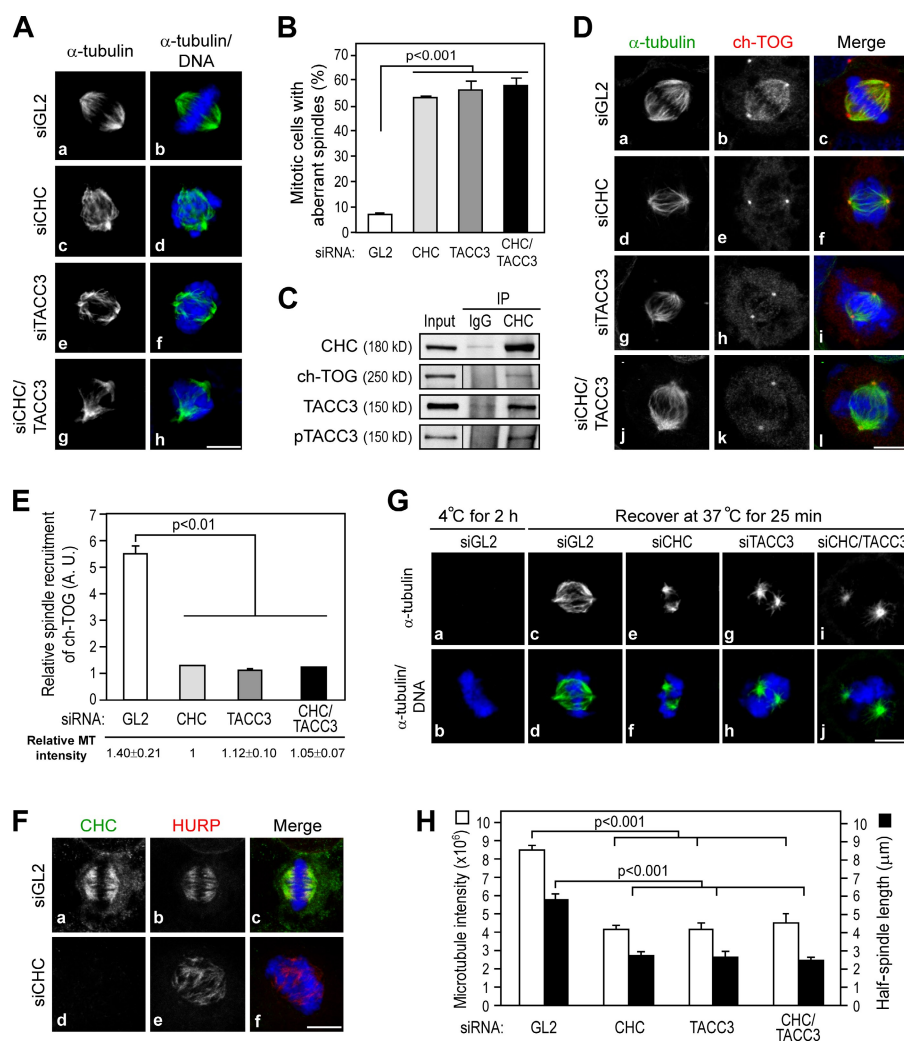
itself does not appear to bind to MTs. Although the B-Myb–filamin complex acting as scaffold proteins to deliver CHC to spindles was proposed, the possibility that the B-Myb target genes may facilitate CHC spindle localization cannot be excluded.

In summary, our data implicate CHC as a key factor, mediating a direct interaction with phospho-S558 TACC3 and recruiting TACC3–ch-TOG to the spindle for MT stabilization. Importantly, these findings link CHC to the complex process of mitotic spindle organization regulated by aurora A.

Materials and methods

Plasmids, siRNAs, and antibodies
The cDNAs coding full-length or domains of TACC3 and CHC (Kazusa DNA Research Institute) were amplified by PCR and cloned into p3×Flag–CMV-7.1, pcDNA3-HA, EGFP-C1, pGEX-4T-1, and pMAL-c2X vectors. S558 mutants were made by site-directed mutagenesis. The siRNA-resistant constructs of Flag- or GFP-tagged CHC WT and Δ(331–542) were generated by two rounds of site-directed mutagenesis to introduce silent mutations (5′-AAGAATCCAATTCGAAGACCAATTTCAGCA-3′ to 5′-AAGAATCCTAT-CAGGCGCCCGATTTCAGCA-3′). GFP-H2B was provided by R.-H. Chen (Academia Sinica, Taipei, Taiwan). Specific siRNA oligonucleotides against TACC3 and CHC (Gergely et al., 2003; Motley et al., 2003) were synthesized by Thermo Fisher Scientific. The following primary antibodies were used: rabbit anti-TACC3 (H-300), mouse anti-TACC3 (D-2), control mouse IgG, and rabbit IgG (Santa Cruz Biotechnology, Inc.); mouse anti-CHC (X22 [EMD] and M23 [BD]); rabbit anti–maltose-binding protein (MBP; Abcam); rabbit anti-phospho–histone H3 (Ser-10) and mouse anti–β-actin (Millipore); mouse anti–α-tubulin, mouse anti–α-tubulin FITC conjugated (DM1A), and mouse anti-Flag (M2; Sigma-Aldrich); rabbit anti–aurora A and phospho-T288 aurora A (Cell Signaling Technology); and mouse anti-HA (Covance). Secondary antibodies used for immunofluorescence labeling were Alexa Fluor 488 chicken anti–mouse IgG, Alexa Fluor 568 goat anti–mouse IgG, and Alexa Fluor 568 goat anti–rabbit IgG (Invitrogen). Both antibodies recognizing pS626 maskin/TACC3 were provided by Y. Arlot-Bonnemains (Pascreau et al., 2005), A. Bird, and A. Hyman (Max Planck Institute, Dresden, Germany; Kinoshita et al., 2005), and the antibody for ch-TOG was provided by L. Cassimeris (Lehigh University, Bethlehem, PA; Cassimeris et al., 2001).

Cell culture, synchronization, drug treatment, and transfection
HeLa cells were maintained in DME supplemented with 10% FBS as described previously (Lin et al., 2006). To generate mitotic extracts, HeLa cells were treated with 100 ng/ml Noc (Sigma-Aldrich) for 16–20 h and collected by shake off. For inhibition of aurora A activity, 2 µM VX-680 was added to the media 2 h before analysis. Transfections of DNA constructs and/or siRNA oligonucleotides were performed using FuGENE 6 (Roche) and Oligofectamine (Invitrogen), respectively. For rescue experiments, siCHC-treated cells transfected with GFP, GFP-CHC WT, or Δ(331–542) were selected by sterile FACS. The selected population, consisting of >90% GFP-expressing cells, was further subjected to analyses of mitotic index and chromosome alignment defect.

Immunoprecipitation, Western blotting, and GST pull-down assays
Cells were resuspended in CSF-XB buffer (Murray, 1991) and lyzed by passing 10× through a 26-G pestle. Lysates were subjected to immunoprecipitation and Western analysis as described previously (Lin et al., 2006). For identification of CHC and domain-mapping experiments, 10 or 4 µg
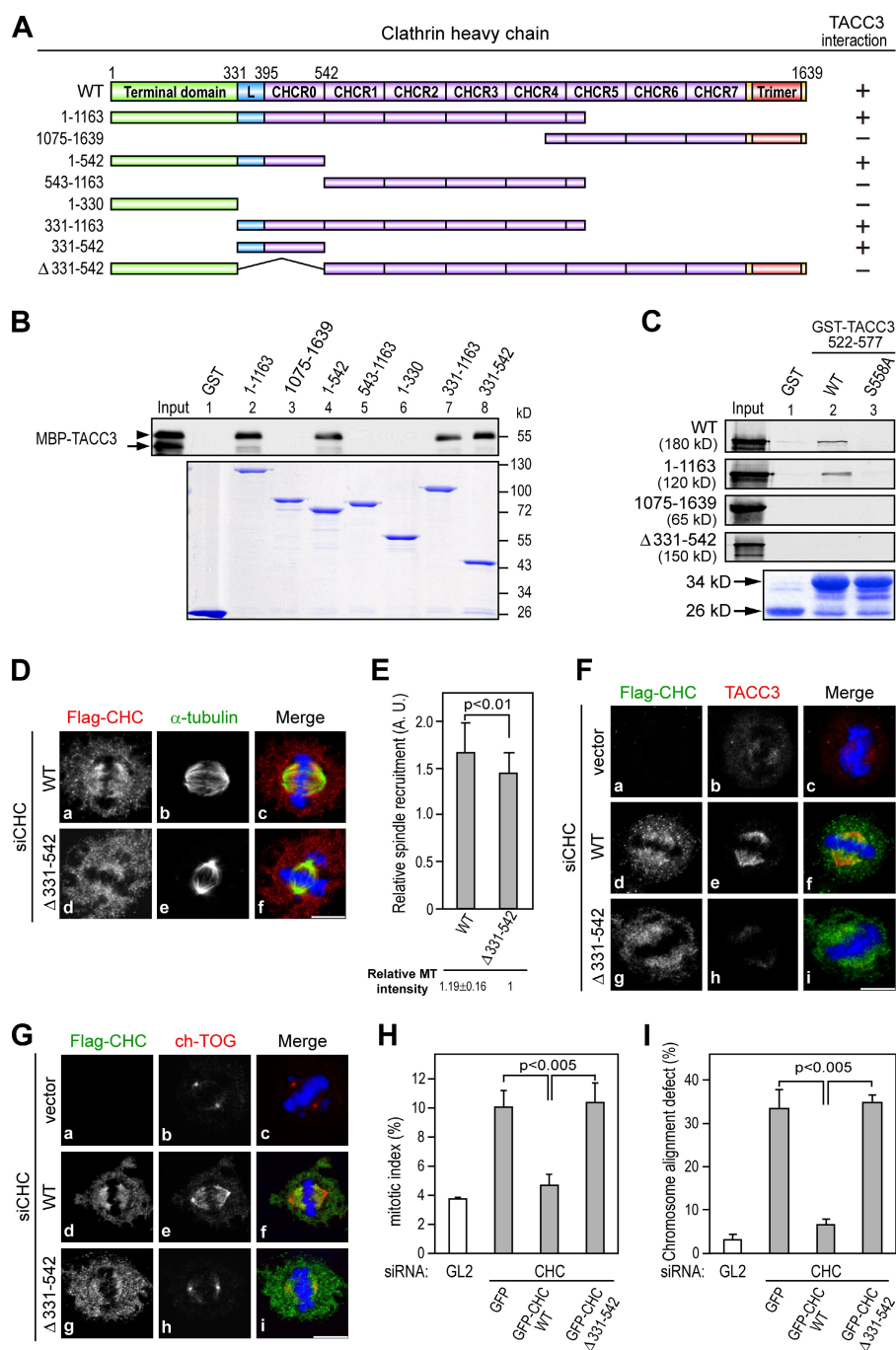
Figure 5. **The CHC 331–542 region is important for TACC3 interaction and spindle recruitment.** (A) A schematic presentation of the CHC domains and deletion mutants used in this study is shown. The interaction of each CHC deletion mutant with TACC3 is indicated. (B) Western blotting shows MBP-TACC3 522–577 recombinant proteins phosphorylated by aurora A and pulled down by the indicated GST fusion proteins. Input represents the 5% amount of MBP-TACC3 protein phosphorylated by aurora A used for each binding reaction and detected by anti-MBP antibody. The arrowhead and arrow indicate phosphorylated and unphosphorylated MBP-TACC3 522–577, respectively. Coomassie blue staining shows the GST fusion proteins used for each binding reaction. (C) Autoradiograph of in vitro ^{35}S-labeled CHC WT or truncated proteins pulled down by GST-TACC3 522–577 proteins being phosphorylated by aurora A. Input and Coomassie blue staining represent 10% of the amount of in vitro–synthesized proteins and GST fusion proteins used for each binding reaction, respectively. (D) Images of HeLa cells treated with siCHC for 6 h and transfected with siCHC-resistant Flag-CHC WT or mutant for an additional 66 h and stained with DNA (blue), α-tubulin (green), and Flag-CHC (red). (E) Histogram shows the relative spindle recruitment of CHC WT or Δ(331–542) in siCHC-treated cells observed in D. The relative spindle MT intensity was normalized against the MT intensity obtained from siCHC and Δ(331–542)-transfected cells (>25 mitotic cells scored per construct). (F and G) Images of HeLa cells transfected with siCHC and the indicated siCHC-resistant Flag-CHC constructs as described in D were stained for Flag-CHC (green), TACC3 (H-300), or ch-TOG (red) and DNA (blue). (H and I) Bar graphs show mitotic index (H) or misaligned chromosomes (I) of HeLa cells transfected with the indicated siRNAs along with siCHC-resistant GFP-CHC constructs (n = 3; mitotic index, >500 cells scored; chromosome alignment defect, ~100 cells scored). Error bars indicate mean ± SD. Bars, 10 µm.

purified GST-TACC3 522–577 WT or S558A protein was phosphorylated by 1 µg recombinant aurora A for 2 h followed by incubation with cell lysates of Noc-treated HeLa cells (~1.5 × 10^7) or indicated in in vitro–synthesized ^{35}S-labeled CHC proteins along with glutathione beads (Thermo Fisher Scientific) in NET-2 buffer (50 mM Tris-HCl, pH 7.5, 150 mM NaCl, and 0.5% NP-40) for an additional 6 h at 4°C. After extensive washing, the resulting bounded proteins were resolved by SDS-PAGE followed by Western or autoradiography analysis or SYPRO ruby staining for further mass spectrometry analysis. Similarly, 2 µg GST-CHC WT or truncated fusion proteins were subjected to binding reaction with 2 µg MBP-TACC3 522–577 fusion proteins phosphorylated by aurora A.

In vitro aster assembly and MT-binding assays
In vitro aster assembly and MT-binding experiments were performed as described previously (Gaglio et al., 1995) with modifications. In brief, after polymerization of MTs, mitotic extracts were centrifuged through a 50% glycerol cushion in KHM buffer at 100,000 g for 30 min at 25°C in a rotor

(TLA100.2; Beckman Coulter). Proteins in the pellet and supernatant were separated by SDS-PAGE followed by Western analysis. For in vitro MT-binding assays, pure bovine brain tubulin (Cytoskeleton, Inc.) was used to generate taxol-stabilized MTs as described previously (Silljé et al., 2006). 2 µg recombinant TACC3 or CHC fusion protein, GST, or MAP proteins with ~70% MAP2 (Cytoskeleton, Inc.) were incubated in BRB80 (80 mM K-Pipes, pH 6.8, 1 mM MgCl$_2$, and 1 mM EGTA) for 25 min at 25°C with or without MTs in a total volume of 25 µl and centrifuged at 100,000 g for 30 min at 25°C in a rotor (TLA100.2). Equal volumes of the pellet and supernatant fractions were separated by SDS-PAGE followed by Coomassie blue staining or Western analysis.

Immunofluorescence and live cell imaging
HeLa cells grown on glass coverslips were fixed (10 min at −20°C methanol), washed with PBS, and incubated with the indicated primary and secondary antibodies (1 h each). DNA was counterstained with DAPI. For cold shock–induced MT depolymerization, siRNA-transfected HeLa cells

were incubated (4°C for 2 h) to completely depolymerize MTs, and MT regrowth was induced by incubating the cells in prewarmed media for the indicated time at 37°C; cells were fixed for immunostaining, mounted in mounting medium (Vector Laboratories), and observed using a confocal microscope (Radiance 2100; Bio-Rad Laboratories) with a Plan Apo VC 100×/1.40 NA oil immersion objective (Nikon) and a confocal system (LSM 510 META; Carl Zeiss, Inc.) with a Plan Apochromat 100× 1.4 NA oil immersion objective (Carl Zeiss, Inc.). ZEN (Carl Zeiss, Inc.) and Meta-Morph (MDS Analytical Technologies) imaging software were used for imaging processing. For live cell imaging, cells grown in a glass-bottom dish (WillCo Wells B.V.) were treated for 48 h with siRNAs and transfected with GFP-H2B to observe chromosome dynamics in living cells. Images were obtained 72–96 h after siRNA treatment in CO_2-independent medium (Invitrogen) and within a heated chamber at 37°C. Images were acquired with an inverted microscope (IX71; Olympus) with a UPlan SApo 40× NA 0.90 objective (Olympus). Voltage5 (PerkinElmer) and MetaMorph imaging software were used to collect and process data, respectively. Images were captured at 5-min intervals for 12 h.

Image quantification and statistical analysis

For quantitative immunostaining experiments, identical laser power and acquisition settings were used for each independent assay, and the mean pixel density of images was measured by MetaMorph imaging software. Relative spindle recruitment was assayed by dividing the mean pixel density measured in 1.01 μm^2 area of interest placed over the spindle by that measured in a region outside the spindle, then further normalizing to the relative spindle MT immunostaining intensity, which was caused by a decreased MT density in siCHC and/or siTACC3-treated cells. Relative spindle MT fluorescence intensity in siRNA-treated cells was calculated from the mean pixel density measured in manually defined area that contained the spindle region in siRNA-treated samples after normalization to the sample with the lowest MT intensity in the same experimental set (taken as one). Half-spindle length was determined from confocal images using the manual line measurement tool in MetaMorph software. The mitotic index was quantified by counting the number of cells in mitosis determined by positive staining of phospho-Ser10 of histone H3 as a fraction of the total number of cells (>500 cells counted per experiment). Statistical significance was ascertained using a Student's t test. In Fig. 3 C, the box in the box and whisker plot represents 50% of all cells from the 25th (bottom line of the box) to 75th percentile (top line). The line in the middle of each box indicates the median. The values that are not outliers are connected to the box with a vertical line, and whiskers, which are ended by a horizontal line, represent the fifth and 95th percentiles. Outliers are indicated by an X outside of the whiskers.

Online supplemental material

Fig. S1 shows that the phosphorylation of S558 by itself is essential for TACC3 spindle localization. Fig. S2 shows the specificity of both antibodies in recognizing phospho-S558 TACC3. Fig. S3 shows that TACC3 and CHC cannot directly bind to MTs. Video 1 shows chromosome segregation in control, CHC, and/or TACC3 siRNA-treated HeLa cells. Video 2 shows that CHC and/or TACC3 siRNA-treated HeLa cells failed to proceed into anaphase for a period of >5 h from chromosome condensation onset. Online supplemental material is available at http://www.jcb.org/cgi/content/full/jcb.200911120/DC1.

References

Barr, A.R., and F. Gergely. 2007. Aurora-A: the maker and breaker of spindle poles. *J. Cell Sci.* 120:2987–2996. doi:10.1242/jcs.013136

Barr, A.R., and F. Gergely. 2008. MCAK-independent functions of ch-Tog/XMAP215 in microtubule plus-end dynamics. *Mol. Cell. Biol.* 28:7199–7211. doi:10.1128/MCB.01040-08

Brittle, A.L., and H. Ohkura. 2005. Centrosome maturation: Aurora lights the way to the poles. *Curr. Biol.* 15:R880–R882. doi:10.1016/j.cub.2005.10.022

Cassimeris, L., D. Gard, P.T. Tran, and H.P. Erickson. 2001. XMAP215 is a long thin molecule that does not increase microtubule stiffness. *J. Cell Sci.* 114:3025–3033.

Gaglio, T., A. Saredi, and D.A. Compton. 1995. NuMA is required for the organization of microtubules into aster-like mitotic arrays. *J. Cell Biol.* 131:693–708. doi:10.1083/jcb.131.3.693

Gergely, F., V.M. Draviam, and J.W. Raff. 2003. The ch-TOG/XMAP215 protein is essential for spindle pole organization in human somatic cells. *Genes Dev.* 17:336–341. doi:10.1101/gad.245603

Giet, R., R. Uzbekov, F. Cubizolles, K. Le Guellec, and C. Prigent. 1999. The *Xenopus laevis* aurora-related protein kinase pEg2 associates with and phosphorylates the kinesin-related protein XlEg5. *J. Biol. Chem.* 274:15005–15013. doi:10.1074/jbc.274.21.15005

Giet, R., D. McLean, S. Descamps, M.J. Lee, J.W. Raff, C. Prigent, and D.M. Glover. 2002. *Drosophila* aurora A kinase is required to localize D-TACC to centrosomes and to regulate astral microtubules. *J. Cell Biol.* 156:437–451. doi:10.1083/jcb.200108135

Hoar, K., A. Chakravarty, C. Rabino, D. Wysong, D. Bowman, N. Roy, and J.A. Ecsedy. 2007. MLN8054, a small-molecule inhibitor of Aurora A, causes spindle pole and chromosome congression defects leading to aneuploidy. *Mol. Cell. Biol.* 27:4513–4525. doi:10.1128/MCB.02364-06

Kinoshita, K., T.L. Noetzel, L. Pelletier, K. Mechtler, D.N. Drechsel, A. Schwager, M. Lee, J.W. Raff, and A.A. Hyman. 2005. Aurora A phosphorylation of TACC3/maskin is required for centrosome-dependent microtubule assembly in mitosis. *J. Cell Biol.* 170:1047–1055. doi:10.1083/jcb.200503023

Kline-Smith, S.L., and C.E. Walczak. 2004. Mitotic spindle assembly and chromosome segregation: refocusing on microtubule dynamics. *Mol. Cell.* 15:317–327. doi:10.1016/j.molcel.2004.07.012

Lee, M.J., F. Gergely, K. Jeffers, S.Y. Peak-Chew, and J.W. Raff. 2001. Msps/XMAP215 interacts with the centrosomal protein D-TACC to regulate microtubule behaviour. *Nat. Cell Biol.* 3:643–649. doi:10.1038/35083033

LeRoy, P.J., J.J. Hunter, K.M. Hoar, K.E. Burke, V. Shinde, J. Ruan, D. Bowman, K. Galvin, and J.A. Ecsedy. 2007. Localization of human TACC3 to mitotic spindles is mediated by phosphorylation on Ser558 by Aurora A: a novel pharmacodynamic method for measuring Aurora A activity. *Cancer Res.* 67:5362–5370. doi:10.1158/0008-5472.CAN-07-0122

Lin, D.Y., Y.S. Huang, J.C. Jeng, H.Y. Kuo, C.C. Chang, T.T. Chao, C.C. Ho, Y.C. Chen, T.P. Lin, H.I. Fang, et al. 2006. Role of SUMO-interacting motif in Daxx SUMO modification, subnuclear localization, and repression of sumoylated transcription factors. *Mol. Cell.* 24:341–354. doi:10.1016/j.molcel.2006.10.019

Marumoto, T., S. Honda, T. Hara, M. Nitta, T. Hirota, E. Kohmura, and H. Saya. 2003. Aurora-A kinase maintains the fidelity of early and late mitotic events in HeLa cells. *J. Biol. Chem.* 278:51786–51795. doi:10.1074/jbc.M306275200

Motley, A., N.A. Bright, M.N. Seaman, and M.S. Robinson. 2003. Clathrin-mediated endocytosis in AP-2–depleted cells. *J. Cell Biol.* 162:909–918. doi:10.1083/jcb.200305145

Murray, A.W. 1991. Cell cycle extracts. *Methods Cell Biol.* 36:581–605. doi:10.1016/S0091-679X(08)60298-8

O'Brien, L.L., A.J. Albee, L. Liu, W. Tao, P. Dobrzyn, S.B. Lizarraga, and C. Wiese. 2005. The *Xenopus* TACC homologue, maskin, functions in mitotic spindle assembly. *Mol. Biol. Cell.* 16:2836–2847. doi:10.1091/mbc.E04-10-0926

Okamoto, C.T., J. McKinney, and Y.Y. Jeng. 2000. Clathrin in mitotic spindles. *Am. J. Physiol. Cell Physiol.* 279:C369–C374.

Pascreau, G., J.G. Delcros, J.Y. Cremet, C. Prigent, and Y. Arlot-Bonnemains. 2005. Phosphorylation of maskin by Aurora-A participates in the control of sequential protein synthesis during *Xenopus laevis* oocyte maturation. *J. Biol. Chem.* 280:13415–13423. doi:10.1074/jbc.M410584200

Peset, I., and I. Vernos. 2008. The TACC proteins: TACC-ling microtubule dynamics and centrosome function. *Trends Cell Biol.* 18:379–388. doi:10.1016/j.tcb.2008.06.005

Peset, I., J. Seiler, T. Sardon, L.A. Bejarano, S. Rybina, and I. Vernos. 2005. Function and regulation of Maskin, a TACC family protein, in microtubule growth during mitosis. *J. Cell Biol.* 170:1057–1066. doi:10.1083/jcb.200504037

Royle, S.J., and L. Lagnado. 2006. Trimerisation is important for the function of clathrin at the mitotic spindle. *J. Cell Sci.* 119:4071–4078. doi:10.1242/jcs.03192

Royle, S.J., N.A. Bright, and L. Lagnado. 2005. Clathrin is required for the function of the mitotic spindle. *Nature.* 434:1152–1157. doi:10.1038/nature03502

Sasai, K., J.M. Parant, M.E. Brandt, J. Carter, H.P. Adams, S.A. Stass, A.M. Killary, H. Katayama, and S. Sen. 2008. Targeted disruption of Aurora A causes abnormal mitotic spindle assembly, chromosome misalignment and embryonic lethality. *Oncogene.* 27:4122–4127. doi:10.1038/onc.2008.47

Schmid, S.L. 1997. Clathrin-coated vesicle formation and protein sorting: an integrated process. *Annu. Rev. Biochem.* 66:511–548. doi:10.1146/annurev.biochem.66.1.511

Schneider, L., F. Essmann, A. Kletke, P. Rio, H. Hanenberg, W. Wetzel, K. Schulze-Osthoff, B. Nürnberg, and R.P. Piekorz. 2007. The transforming acidic coiled coil 3 protein is essential for spindle-dependent chromosome alignment and mitotic survival. *J. Biol. Chem.* 282:29273–29283. doi:10.1074/jbc.M704151200

Silljé, H.H., S. Nagel, R. Körner, and E.A. Nigg. 2006. HURP is a Ran-importin beta-regulated protein that stabilizes kinetochore microtubules in the vicinity of chromosomes. *Curr. Biol.* 16:731–742. doi:10.1016/j.cub.2006.02.070

Wong, J., R. Lerrigo, C.Y. Jang, and G. Fang. 2008. Aurora A regulates the activity of HURP by controlling the accessibility of its microtubule-binding domain. *Mol. Biol. Cell.* 19:2083–2091. doi:10.1091/mbc.E07-10-1088

Yamauchi, T., T. Ishidao, T. Nomura, T. Shinagawa, Y. Tanaka, S. Yonemura, and S. Ishii. 2008. A B-Myb complex containing clathrin and filamin is required for mitotic spindle function. *EMBO J.* 27:1852–1862. doi:10.1038/emboj.2008.118